

PYROLYTIC GRAPHITE AS AN EFFICIENT SECOND-ORDER NEUTRON FILTER AT TUNED POSITIONS OF BOUNDARY CROSSING

© 2010 M. Adib, A. Abdel Kawy, N. Habib, M. El Mesiry

Reactor Physics Department, Nuclear Research Center, Egyptian Atomic Energy Authority, Cairo, Egypt

An investigation of pyrolytic graphite (PG) crystal as an efficient second order neutron filter at tuned boundary crossings has been carried out. The neutron transmission through PG crystal at these tuned crossing points as a function of first- and second-order wavelengths were calculated in terms of PG mosaic spread and thickness. The filtering features of PG crystals at these tuned boundary crossings were deduced. It was shown that, there are a large number of tuned positions at double and triple boundary crossings of the curves (*hkl*) are very promising as tuned filter positions. However, only fourteen of them are found to be most promising ones. These tuned positions are found to be within the neutron wavelengths from 0.133 up to 0.4050 nm. A computer package GRAPHITE has been used in order to provide the required calculations in the whole neutron wavelength range in terms of PG mosaic spread and its orientation with respect to incident neutron beam direction. It was shown that 0.5 cm thick PG crystal with angular mosaic spread of 2° is sufficient to remove 2nd-order neutrons at the wavelengths corresponding to the positions of the intersection boundaries curves (*hkl*).

Keywords: pyrolytic graphite, neutron filter, 2nd-order neutrons, mosaic spread.

Introduction

PG has been in use for about 30 years as a filter. Since in PG, crystallites are preferentially oriented along the hexagonal *c*-axis. The transmission of neutrons thru PG with *c*-axis parallel to the beam versus neutron wavelength, exhibits "absorption" lines due to Bragg scattering. By applying PG as second-order filter in neutron powder diffractometry, Loopstra [2] and Shapiro [3] demonstrated its high efficiency for first-order neutrons with $\lambda = 0.26$ nm. Recently Adib et al. [4] showed that five centimeters thick low quality PG (mosaic 8°) cooled to liquid nitrogen temperature is a high efficiency for transmitting first-order of (4-7 meV) and (10-15 meV) neutrons incident along its *c*-axis.

However, Frikkee [5] reported an investigation that has been carried out on the neutron transmission through a PG filter as a function of the filter orientation with respect to the beam. It is shown that highly aligned PG may be tuned for optimum scattering of second-order neutrons in the wavelength range between 0.112 nm and 0.425 nm, by adjusting the filter in an appropriate orientation.

The measurement of neutron transmission through highly oriented (0.4° FWHM on mosaic spread) 1.85 mm thick crystal set at different angles to the incident beam, reported by Mildner et al. [6], was found to justify the existence of the tuned intervals reported by Frikkee [5].

However, the effect of crystal mosaic spread value upon the width of the tuned intervals nor the filtering factors are not investigated. Furthermore, the optimum thickness of PG crystal to be used as high efficient second-order filter was not also estimated.

Recent calculations of the neutron transmission

through PG crystals in terms of mosaic spread, optimum filtering thickness and its orientation with respect to the beam were carried out by Adib et al. [7, 8]. They showed that highly oriented PG crystal having few centimeters thick is an efficient 2nd-order neutron filter within favorable selected intervals covering wavelength band from 0.112nm - 0.425 nm. Such PG crystals if available are expensive. Moreover, the whole selected interval of 2nd-order neutrons, as in case of triple axis neutron spectrometer is not required to carry out the experiment but only at a few fixed values of neutron wavelengths.

Therefore, in the present work, a feasibility study is carried on using less oriented and thinner PG crystals to almost eliminate 2nd-order neutrons at only tuned neutron wavelengths corresponding to the boundary crossings of the curves (*hkl*).

Theoretical treatment

The graphite absorption cross-section due to nuclear capture is very small (≈ 3 mb at $E_n = 0.025$ eV). Therefore the total cross-section is given by

$$\sigma = \sigma_{ids} + \sigma_{Bragg} \tag{1}$$

where σ_{ids} is the thermal diffuse scattering and σ_{Bragg} correspond to Bragg scattering cross-section due to reflection from (*hkl*) planes.

As shown by Freund [9] σ_{ids} can be split into σ_{mph} (multiple phonon) and σ_{sph} (single phonon) depending on neutron energy. However, M. Adib [7] showed that best fit of the multi-phonon scattering

cross-section term given by Freund [9] in the range $E \gg K_B\theta$ can be replaced by: the static incoherent approximation reported by Cassels [10].

Following Frikkee [5], in PG the crystallites are aligned to a high degree with their hexagonal c-axes parallel, whereas the a-axes are oriented at random. In the case of perfect alignment of the c-axes, the lattice planes (hkl) are tangent to a cone with its axis along the c-direction and an apex angle θ_{hkl} determined by

$$\sin\theta_{hkl} = \frac{l}{c} d_{hkl}, \quad (2)$$

where d_{hkl} is interplanar distance.

As shown by Frikkee [5] that, it is possible to tune the PG plates for optimum scattering of second-order neutrons in a continuous wavelength range by varying the angle between the c-direction and the incident neutron beam.

If this angle is denoted by ψ , and if the mosaic spread is negligible in comparison with ψ , the lattice planes (hkl) will scatter neutrons in the following wavelength intervals:

$$\begin{aligned} 2d_{hkl} \sin(\theta_{hkl} - \psi) \leq \lambda \leq 2d_{hkl} \sin(\theta_{hkl} + \psi) \text{ for } \theta_{hkl} \geq \psi, \\ 0 \leq \lambda \leq 2d_{hkl} \sin(\theta_{hkl} + \psi) \text{ for } \theta_{hkl} \leq \psi. \end{aligned} \quad (3)$$

The planes ($00l$), on the other hand, scatter neutrons with a discrete wavelength $\lambda = 2d_{00l} \cos\psi$.

The Bragg scattering cross-section due to reflection from ($00l$) planes of PG is given by K. Naguib and M. Adib [11] as

$$\sigma_{Bragg}(00l) = -\frac{1}{Nt_o} \ln(1 - P_{00l}), \quad (4)$$

where N is the number of unit cell/cm³, t_o is the effective thickness and P_{00l} is the reflecting power [4].

However, it was shown by Frikkee [5] that the scattering cross-section due to non- $00l$ planes reaches pronounced maximum at the boundaries in the $(\lambda; \psi)$ plane given by

$$\lambda^\pm = 2d_{hkl} \sin|\theta_{hkl} \pm \psi|. \quad (5)$$

Following, Adib et al. [7] The Bragg scattering cross-section due to reflection from non- $00l$ planes of PG crystal with standard deviation η on mosaic blocks, and set at angle ψ , at wavelength λ in the interval between λ^- **Error! Bookmark not defined.**

and λ^+ , can be given as

$$\sigma_{Bragg}^{non-00l} = \frac{N_o \lambda^3 F_{hkl}^2 e^{-2w}}{4d_{hkl} \sin\psi \cos\theta_{hkl} \left| \lambda - \lambda_{hkl}^\pm \right|^2}, \quad (6)$$

where, F_{hkl} is the structure factor of the unit cell and e^{-2w} is the Debye - Waller factor [12].

While at $\lambda \leq \lambda^-$ and $\lambda \geq \lambda^+$ the Bragg scattering cross-section is decreased due to mosaic spread and can be expressed as

$$\sigma_{Bragg}^{non-00l} = \frac{N_o \lambda^3 F_{hkl}^2 e^{-2w} W(\Delta)}{4d_{hkl} \sin\psi \cos\theta_{hkl} (\delta\lambda)^2}, \quad (7)$$

where $W(\Delta)$ is the Gaussian distribution of the graphite having η standard deviation of its mosaic blocks [12].

Consequently, the Bragg scattering of PG crystal set at angle ψ versus wavelength due to reflections from (hkl) planes can be given as

$$\sigma_{Bragg} = \sigma_{Bragg}^{00l} + \sum_{hkl} \sigma_{Bragg}^{non-00l}, \quad (8)$$

where, summation is taken over all non- $(00l)$ planes satisfying the inequalities given by Eq. (3).

A Computer package GRAPHITE has been developed by Adib and Fathalla [13] in order to calculate the total cross section and transmission of neutrons of energy range from 0.1 meV to 10 eV through crystalline graphite. Where the main graphite physical parameters required for calculations are taken the same as given in Ref. [13].

Features of PG crystals as a 2nd-order neutron filter

The total effect of the various Bragg reflections, with exception of ($00l$) reflections, is, that neutrons in the short-wave-length region bounded by the maximum value of $2d_{hkl} \sin(\theta_{hkl} + \psi)$, will be removed to some extent from the beam. On the other hand, the filter should be transparent for first-order neutrons. This region was found [5] to cover the wave-length interval $0.112 \text{ nm} < \lambda/2 < 0.425 \text{ nm}$.

The possibility to tune a PG filter is a consequence of the fact that the scattering cross section due to the (hkl) planes reaches pronounced maxima at the boundaries in the (λ, ψ) plane given by equation (3). Hence, one may expect to realize optimum scattering of neutrons by the (hkl) planes at the boundary curves $(hkl)^\pm$ in (λ, ψ) space defined by equation (3). Possible tuned positions of second-

order neutrons are calculated and displayed in Fig. 1.

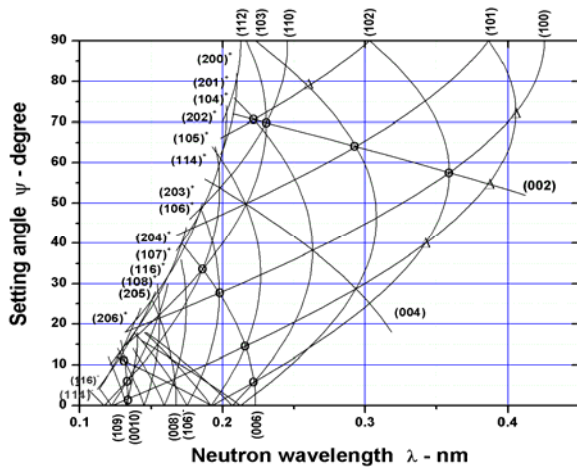


Fig. 1. Tuning diagram for PG filter.

Table 1. Tuned positions at boundary crossing points

Intersection	Ψ_0 , deg		$2nd - order(\lambda_{1/2} - nm)$	
	Present work	Frikkee [5]	Present work	Frikkee [5]
(100)-(101) ⁺	72.35	-	0.4050	-
(101) ⁺ -(002)	54.76	-	0.3864	-
(100)-(102) ⁺ -(002)	57.57	-	0.3591	-
(101) ⁺ -(102) ⁺	39.95	-	0.3422	-
(103) ⁺ -(101) ⁻ -(002)	64.00	64.02	0.2936	0.2935
(103) ⁺ -(102) ⁻	78.81	-	0.2599	-
(110) ⁺ -(112) ⁺ -(002)	69.86	69.88	0.2306	0.2305
(104) ⁺ -(102) ⁻ -(002)	70.63	-	0.2221	-
(102) ⁺ -(104) ⁺ -(006)	5.78	-	0.2221	-
(101) ⁺ -(105) ⁺ -(006)	14.57	14.62	0.2160	0.2161
(100)-(106) ⁺ -(006)	27.68	-	0.1976	-
(112) ⁺ -(114) ⁺ -(006)	33.60	33.65	0.1859	0.1859
(101) ⁺ -(109) ⁺ -(0010)	1.66	1.70	0.1339	0.1340
(114) ⁺ -(116) ⁺ -(0010)	6.00	6.07	0.1332	0.1333

Determination of PG filtering efficiency at tuned intersection points

To study the PG filtering efficiency of 2nd-order neutrons at tuned points given in Table 1, the poisons at boundary crossing $(hkl)^\pm$ curves were calculated at different setting angles ψ around the intersection position. The optimum setting angle ψ_0 within an accuracy of 0.01 degree, at which the wavelengths at boundary crossings of different $(hkl)^\pm$ curves are coincident with each others, were determined. Then, the neutron transmissions through 1 cm thick PG crystal having different mosaic spread values and set at the optimum angle ψ_0 were calculated as a function of λ around the boundaries crossing point with step of $\delta\lambda = 0.001$ nm. Consequently the neutron wavelength at this minimum transmission which corresponds to $(\lambda_{1/2})$ is determined. Using the same PG parameters, the neutron transmissions at double wavelength (i.e. at λ) were also calculated.

A striking systematic feature of Fig. 1 is the large number of intersection points of the curves $(hkl)^\pm$ and $(00l)$. As shown by Frikkee [5] that these intersections occur for the combinations: $(hkl)^\pm - (hkl')^\pm - (00l \pm l')$ and are independent of the c/a ratio. However, Frikkee [5] neglected some triple points and also all double ones. The most efficient intersections as promising 2nd-order filter are listed in Table 1 along with those reported by Frikkee [5].

It may be noticed that the intersection points of $(hkl)^\pm$ planes at boundaries with curves (004) and (008) reflections fail as 2nd-order neutron filter, because the, 1st-order ones are scattered by the reflections from (002) and (004) planes respectively.

Filtering efficiency of PG at tuned double intersection points

The result of calculations for double intersection points (100) - (101)⁺, (101)⁺ - (002) and (101)⁺ - (102) are displayed in Fig. 2, a, b, c respectively.

Fig. 2, a and c show that, the shape of the dip in transmission curve as a function of wavelength $(\lambda_{1/2})$ at the boundary crossing, are asymmetric and moreover, its width is slightly broadened with increasing the PG mosaic spread. While, the neutron transmission at 1st-order λ , is almost constant. Such behavior is in agreement with the measurements carried out by Mildner et al. [6]. While Fig. 2, b shows that, the shape of the dip at double crossing point (101)⁺-(002) is almost symmetric and its width is increasing with the increase of η . From Fig. 2 one can observe that, the neutron transmission at the boundary crossing $(\lambda_{1/2})$ is decreased by one order, while at the 1st-order (λ) the transmission is almost

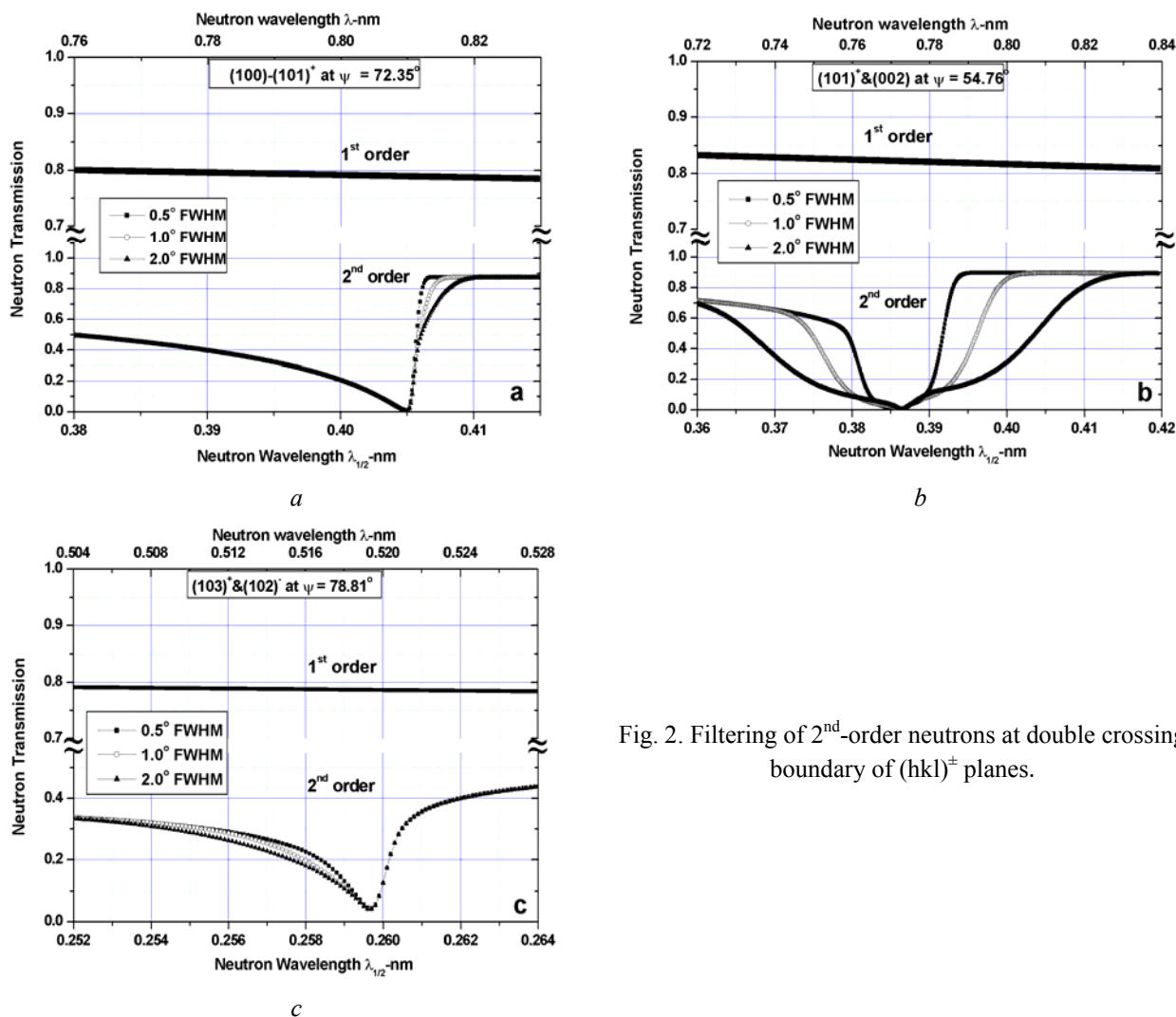


Fig. 2. Filtering of 2nd-order neutrons at double crossing boundary of (hkl)[±] planes.

constant and higher than 90 % Therefore PG crystal at double boundary crossing points can be efficiently used as 2nd-order neutron filter. From Fig. 2, the

FWHM of the dips $\Delta \lambda$ at boundaries for various η are determined and listed in Table 2.

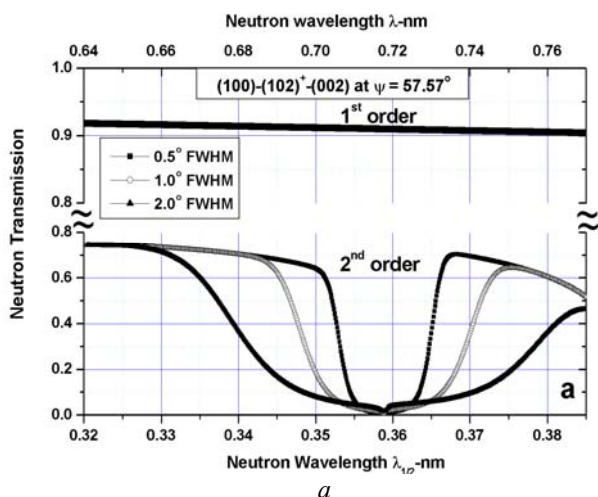
Table 2. Filtering features of PG crystal at boundary crossing points

Position at boundary crossings ($\lambda_{1/2}$, nm)	$\Delta \lambda_{1/2}$, nm			Thickness t_{10} , cm			T(t_{10}) of 1 st -order λ , %		
	$\eta = 0.5^\circ$	1°	2°	0.5°	1°	2°	0.5°	1°	2°
0.4050	0.0084	0.0090	0.0095	0.40	0.42	0.44	92.80	92.50	92.35
0.3864	0.0108	0.0187	0.0308	0.10	0.15	0.21	99.06	98.60	98.05
0.3591	0.0122	0.0222	0.0400	0.17	0.25	0.42	97.99	97.05	95.10
0.3422	0.0024	0.0028	0.0032	0.78	0.78	0.78	95.18	95.18	95.18
0.2935	0.126	0.0223	0.0385	0.16	0.22	0.30	98.07	97.35	96.41
0.2599	0.0018	0.0022	0.0025	0.89	0.89	0.89	83.86	83.86	83.86
0.2306	0.0129	0.0217	0.0289	0.18	0.23	0.31	97.74	97.12	96.14
0.2221	0.00935	0.0129	0.01315	0.22	0.35	0.47	95.59	93.08	88.25
0.2221	0.00048	0.00083	0.00135	0.25	0.37	-	98.93	98.43	-
0.2160	0.0013	0.0020	0.003	0.53	0.60	0.74	97.74	97.45	96.86
0.1976	0.0015	0.0026	0.0044	1.00	1.40	2.00	95.66	93.78	91.52
0.1859	0.0021	0.0031	0.0043	0.48	0.56	0.64	97.84	97.49	97.14
0.1339	0.00028	0.00028	-	0.97	0.89	-	89.39	90.22	-
0.1332	0.00066	0.00074	-	0.42	0.44	-	95.15	94.93	-

In most cases, to carry out neutron diffraction experiments, it is sufficient to select the thickness t_{10} that attenuates the 2nd-order neutrons by factor of ten [14] and the transmission $T(t_{10})$ at the 1st-order one to be high enough. Thickness t_{10} and $T(t_{10})$ of PG having different η at boundary crossing points were determined and listed in Table 2.

Filtering efficiency of PG at tuned triple intersection points with (002)

The neutron transmission through 1 cm thick PG crystal having different η and set at optimum angle



ψ_0 were calculated as a function of λ around the triple boundaries crossing points $(100)-(102)^+-(002)$ and $(103)^+-(101)^--(002)$ and displayed in Fig. 3, *a* and *b* respectively.

It could be observed that shapes of the dip in the transmission curve are symmetric and their widths increase with the increase of η . Moreover, the neutron transmission at the dips (i.e. $\lambda_{1/2}$) are less than 0.004 while at λ are more than 0.98. Therefore a thinner (less than 1 cm) and low quality (η more than 2°) PG crystal can be efficiently used as 2nd-order neutron filter at these triple crossing points.

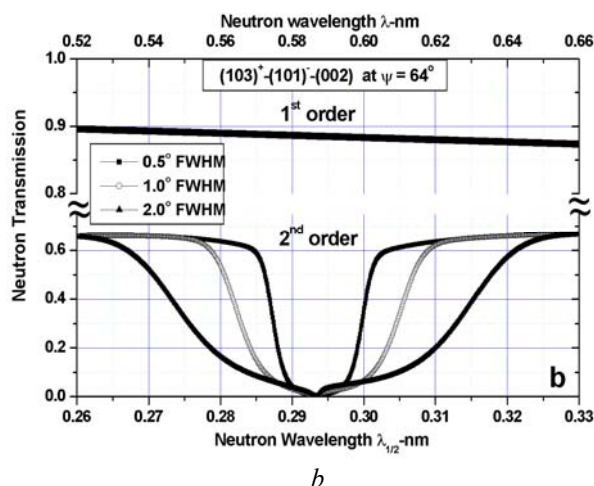


Fig. 3. Neutron Transmission through PG at tuned triple intersection points with (002).

Filtering efficiency of PG at tuned triple intersection points with (006)

Similar calculation of the neutron transmission as a function of λ around the triple boundaries crossing points $(102)^+-(104)^+-(006)$ and $(101)^+-(105)^+-(006)$ are carried out. The results are displayed in Fig. 4, *a* and *b* respectively.

From Fig. 4, one can also notice the behavior of the transmission curve at the triple crossing points $(101)^+-(105)^+-(006)$ and $(112)^+-(114)^+-(006)$ are the same as at $(100)-(102)^+-(002)$ and $(103)^+-(101)^--(002)$ triple crossing points. However, at triple crossing boundaries with (006) even more thinner PG crystals may be selected.

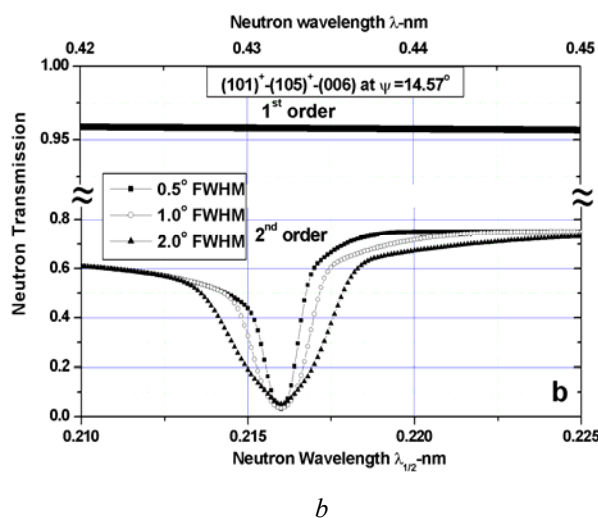
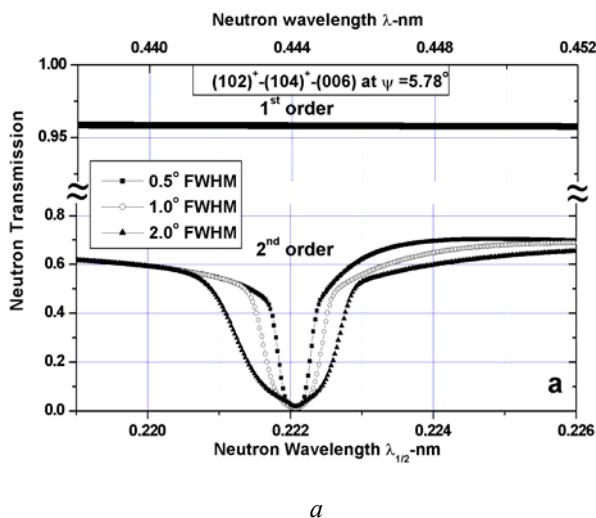


Fig. 4. Filtering of 2nd neutrons at triple crossing boundary of curve (006).

Filtering efficiency of PG at tuned triple intersection points with (0010)

The results of calculation of the neutron transmissions at triple crossings boundaries $(101)^+-(109)^+-(0010)$ and $(114)^+-(116)^+-(0010)$, are

displayed in Fig. 5, *a* and *b* respectively. Fig. 5 shows that at these triple crossings boundaries, the selected PG crystals must be highly oriented ($\eta < 2^\circ$). This is due to the fact that the setting angles at these triple crossing points are close to zero.

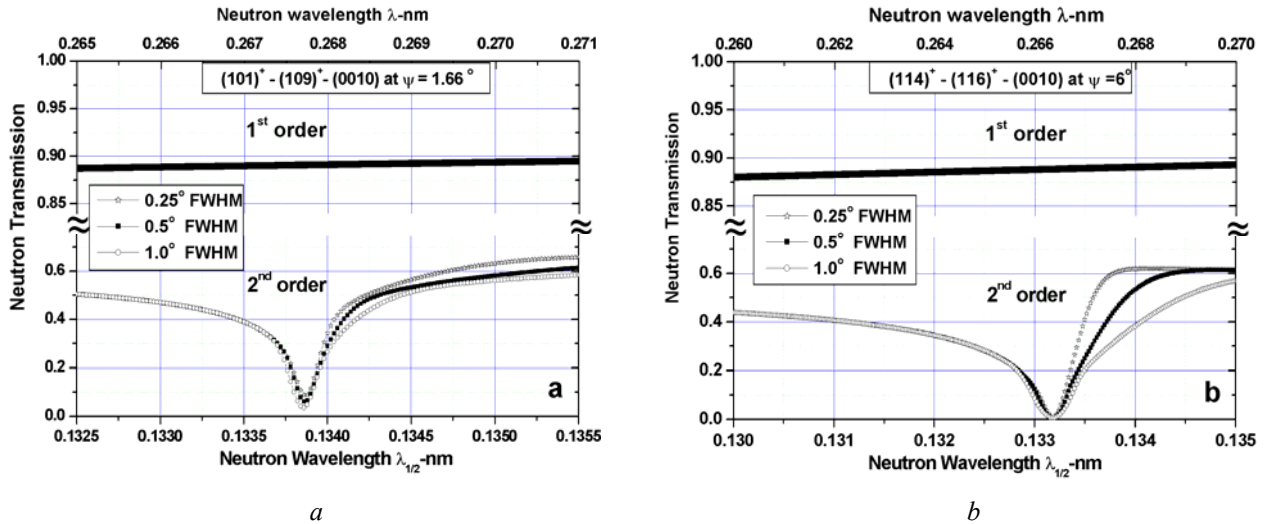


Fig. 5. Filtering of 2nd-neutrons at triple crossing boundary of curve (0010).

The poisons at the selected fourteen boundary crossing points along with their widths $\Delta\lambda_{1/2}$, t_{10} and $T(t_{10})$ for different η are calculated and listed in Table 2.

The neutron transmissions $T(t_{10})$ at 1st-order λ Table 2 shows that, a thinner and less oriented bulk PG crystal can be used as an efficient 2nd-order neutron filter at the wavelengths corresponding to the poison of the intersection boundaries points.

However, the first four crossing points (listed in Table 2) lies in wavelength band $\frac{1}{2}\lambda_{cut\ off} \leq \lambda \leq$

$\leq \lambda_{cut\ off}$, where $\lambda_{cut\ off}$ is Bragg cut off wavelength of polycrystalline graphite (0.667 nm). While from the second to the ninth lies in band of polycrystalline Be (0.396 nm). Since polycrystalline graphite or Be is much cheaper than PG, therefore, the calculation of t_{10} and $T(t_{10})$, for cooled to liquid nitrogen temperature polycrystalline graphite and Be are carried out [14], neglecting the contribution of SANS cross section in a large powdered samples having pores. Such contribution may strongly decrease the transmission of 1st-order neutrons [15].

The results of these calculations are listed in Table 3 along with those for PG having $\eta = 1^\circ$.

Table 3. Filtering features of PG, Be and graphite crystals

$\lambda_{1/2}$, nm	t_{10} , cm at $\lambda_{1/2}$			$T(t_{10})$ at 1 st -order λ , %		
	PG	Be	Graphite	PG	Be	Graphite
0.4050	0.40	-	3.9	92.80	-	63.77
0.3864	0.15	9.8	4.4	98.60	49.40	84.50
0.3591	0.25	11.0	4.3	97.05	47.77	85.74
0.3422	0.78	2.0	5.0	95.18	87.94	84.26
0.2935	0.22	2.4	-	97.35	87.45	-
0.2599	0.89	2.5	-	83.86	88.18	-
0.2306	0.23	2.8	-	97.12	87.99	-
0.2221	0.35	2.4	-	93.08	89.89	-
0.2221	0.37	2.4	-	98.43	89.89	-
0.2160	0.60	2.5	-	97.45	89.69	-

Table 3 shows that, the thickness t_{10} of PG is much thinner than that for polycrystalline graphite or Be and providing more higher transmission of

1st-order than them. The final choice depends upon the experimental requirements and the price.

Conclusions

As a result, one can conclude that, a thinner ($t_{10} \leq 0.5$ cm) and less oriented bulk PG crystals ($\eta \geq 2^\circ$)

can be used as an efficient 2nd-order neutron filter at the wavelengths corresponding to the poisons of the intersection boundaries curves listed in Table 2.

REFERENCES

1. *Kostorz G.* Treatise on Material Science and Technology. Vol. 15. - France, Grenoble: Academic Press, 1979. - 462 p.
2. *Loopstra B.O.* // Nucl. Instrum. & Methods. - 1966. - Vol. 44. - P. 181 - 186.
3. *Shapiro S.M., Chesser N.J.* Characteristics of pyrolytic graphite as an analyzer and higher order filter in neutron scattering experiments // Nucl. Instrum. & Methods. - 1972. - Vol. 101. - P. 183 - 186.
4. *Adib M., Habib N., Fathalla M.* Neutron transmission through pyrolytic graphite crystals // Annals of Nuclear Energy. - 2006. - Vol. 33. - P. 627 - 632.
5. *Frikkee E.* Application of pyrolytic graphite as a tunable neutron filter // Nucl. Instr. & Meth. - 1975. - Vol. 125. - P. 307 - 312.
6. *Mildner, D.F.R., Arif, M., Werner S.A.* // J. Applied Crystallography. - 2001. - Vol. 34. - P. 255 - 262.
7. *Adib M., Habib N., Fathalla M.* Pyrolytic graphite as a selective neutron filter // Nuclear Physics and Atomic Energy. - 2006. - No. 2 (18). - P. 135 - 141.
8. *Adib M., El-Mesiry M.S.* Application of crystalline graphite as a selective thermal neutron filter // Proc. of the 2-nd Int. Conf. "Current Problems in Nuclear Physics and Atomic Energy", Ukraine, Kyiv, 9 - 15 June 2008. - Kyiv, 2009. - P. 516 - 522.
9. *Freund A.K.* Cross-sections of materials used as neutron monochromators and filters // Nucl. Inst. & Meth. - 1983. - Vol. 213. - P. 1553.
10. *Cassels J.M.* // Prog. Nucl. Phys. - 1950. - Vol. 1. - P. 185.
11. *Naguib K., Adib M.* Parasitic neutron Bragg reflections from large imperfect single crystals // Ann. Nucl. Energy. - 1998. - Vol. 25. - P. 1553 - 1563.
12. *Bacon G.E.* Neutron Diffraction / 3-rd edition. - Oxford: Clarendon Press, 1975. - 636 p.
13. *Adib M., Fathalla M.* Computer package for graphite total cross-section calculations // Proc. 6th Nuclear and Particle Physics Conf. / Ed. by M.N.H. Comsan. - Egypt, Luxor, 2007. - P. 35 - 42.
14. *Habib N.* Polycrystalline beryllium and graphite as cold neutron filters // J. of Nuclear and Radiation Physics. - 2006. - Vol. 1, No. 2. - P. 137 - 145.
15. *Gould C.R., Hawari A.I., Sharapov E.I.* Reanalysis of recent neutron diffusion and transmission measurements in nuclear graphite // Nuclear Science and Engineering. - 2010. - Vol. 165. - P. 1 - 10.

ПРОЛІТИЧНИЙ ГРАФІТ ЯК ЕФЕКТИВНИЙ НЕЙТРОННИЙ ФІЛЬТР ДРУГОГО ПОРЯДКУ ПРИ ФІКСОВАНИХ ПОЗИЦІЯХ ПЛОЩИН ПЕРЕТИНУ

М. Адіб, А. Абдель Каві, Н. Хабіб, М. Ель Мезірі

Виконано дослідження кристалів піролітичного графіту (PG) в якості ефективного нейтронного фільтра другого порядку при ослабленні в точках на перетині площин. Пропускання нейтронів через кристал PG у цих точках, як функції довжин хвиль першого та другого порядків було розраховано залежно від мозаїчного розкиду PG та товщини. Було досліджено фільтруючі можливості кристалів PG у вказаних точках. Показано, що існує велика кількість точок послаблення при подвійних та потрійних перетинах площин (hkl), які перспективні як точки фільтрації. Проте тільки 14 з них визнано найбільш перспективними. Визначено точки послаблення для довжин хвиль нейтронів від 0,133 до 0,4050 нм. Пакет комп'ютерних програм GRAPHITE використано для виконання необхідних розрахунків в усьому діапазоні довжин хвиль нейтронів залежно від мозаїчного розкиду PG та його орієнтації відносно до напрямку нейтронного пучка. Показано, що кристал PG товщиною 0,5 см із кутовим мозаїчним розкидом 2° достатній для видалення нейтронів другого порядку при довжинах хвиль, що відповідають точкам перетину кристалічних площин (hkl).

Ключові слова: піролітичний графіт, нейтронний фільтр, нейтрони другого порядку, мозаїчний розкид.

ПИРОЛИТИЧЕСКИЙ ГРАФИТ КАК ЭФФЕКТИВНЫЙ НЕЙТРОННЫЙ ФИЛЬТР ВТОРОГО ПОРЯДКА ПРИ ФИКСИРОВАННЫХ ПОЗИЦИЯХ ПЛОСКОСТЕЙ ПЕРЕСЕЧЕНИЯ

М. Адиб, А. Абдель Кави, Н. Хабиб, М. Эль Мезири

Выполнено исследование кристаллов пиrolитического графита (PG) как эффективного нейтронного фильтра второго порядка при ослаблении в точках пересечения плоскостей. Пропускания нейтронов через кристалл PG в этих точках, как функции длин волн первого и второго порядков было рассчитано в зависимости от мозаичного разброса PG и толщины. Были исследованы фильтрующие возможности кристаллов PG в указанных точках. Показано, что существует большое количество точек ослабления при двойных и тройных пересечениях плоскостей (hkl), которые перспективны как точки фильтрации. Однако только 14 из них признаны наиболее перспективными. Определены точки ослабления для длин волн нейтронов от 0,133 до 0,4050 нм. Пакет компьютерных программ GRAPHITE использовался для проведения необходимых расчетов во

всем диапазоне длин волн нейтронов в зависимости от мозаичного разброса PG и его ориентации относительно направления нейтронного пучка. Показано, что кристалл PG толщиной 0,5 см с угловым мозаичным разбросом 2° достаточен для устранения нейтронов второго порядка при длинах волн, соответствующих точкам пересечения кристаллических плоскостей (hkl).

Ключевые слова: пиролитический графит, нейтронный фильтр, нейтроны второго порядка, мозаичный разброс.

Received 12.05. 10,
revised - 14.10.10.